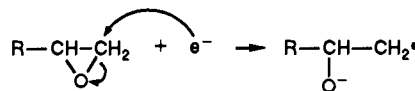


$\pm 120^\circ$, respectively, about the p_x orbital. Figure 8C shows the conformation of the anion radical **3** indicated by the methylene proton coupling constants.

Figure 9A shows the ESR spectrum (the X region) obtained when the Na/propylene oxide (2%)/Ar system deposited with the window covered was subsequently irradiated with 600-nm light for 4 min. The outer sections of the spectrum where only anion radicals **3** contribute were examined with higher instrument gain ($\times 4$) as shown. Figure 9B is the spectrum simulated for a mixture of the two conformers of anion radicals **4** and anion radicals **3** elaborated above. The abundance ratio of 1.0/2.0/0.3 for radicals **4** of large β -proton coupling constant, radicals **4** of small β -proton coupling constant, and radicals **3**, respectively, was assumed. The outer sections of the simulated spectrum were also shown expanded vertically. Based on these analyses we conclude that propylene oxide, on capture of an electron, undergoes a ring-opening process where the external C-O bond is cleaved preferentially ($\sim 90\%$).

Experimental results obtained for 1,2-epoxybutane (Figure 5) and glycidyl methyl ether (Figure 6) indicate that the probability

for the cleavage of the internal C-O bond diminishes further with increasing size of substituent at the β carbon. Ring opening of small cyclic ethers (ethylene oxide and trimethylene oxide) by nucleophilic reagents is well known.¹⁴ When the system is unsymmetrically substituted, the nucleophilic attack occurs at the primary carbon in the majority of cases and is ascribed to a S_N2 -type concerted process. The observed dissociative electron capture process of the epoxy system requires little atomic displacement, but some change in the disposition of valence electrons. It is probable that, influenced by the electron-donating property of the alkyl substituent, the electron capture and ring-opening process occur in a concerted manner as depicted below.



(14) See, for example: Roberts, J. D.; Caserio, M. *Basic Principles of Organic Chemistry*; Benjamin: Reading, MA, 1977; pp 659-665.

Proton NMR Study of the Heme Rotational Mobility in Myoglobin: The Role of Propionate Salt Bridges in Anchoring the Heme

Gerd N. La Mar,* Jón B. Hauksson, L. B. Dugad, Paul A. Liddell, Nittala Venkataramana, and Kevin M. Smith

Contribution from the Department of Chemistry, University of California, Davis, California 95616. Received August 10, 1990

Abstract: The ^1H NMR spectra of the metcyano complexes of the reconstruction products with sperm whale apomyoglobin with the four coprohemin-type isomers, members of the series (propionate) $_n$ (methyl) $_{8-n}$ porphine-iron(III) with $n = 4$ with one propionate on each pyrrole, have been recorded and analyzed. Three of the coprohemin reconstituted cleanly at acidic pH to yield holoproteins with molecular/electronic structures minimally perturbed from those of the native protein; coprohemin IV failed to exhibit detectable incorporation into the heme pocket. Nuclear Overhauser effect spectra provided the unique orientation of the three coprohemin in the pocket, with the nonnative protonated propionates preferring to replace one or both vinyls and tolerating the replacement of one, but not two, interior methyl groups within the folded holoprotein. At alkaline pH, deprotonation of one of the interior propionates leads to spontaneous dissociation into hemin and apomyoglobin. The heme methyls of centrosymmetric coprohemin I and II complexes of sperm whale metMbCN, as well as the sperm whale and horse myoglobin complexes of centrosymmetric dipropionate, hexamethyl hemin, exhibited temperature-dependent saturation transfer among symmetry-related hemin methyls in the holoprotein that can be traced to rotational "hopping" of the hemin about an intact iron-His F8 bond. Measurement of the saturation factors and selective relaxation rates yields hopping rates of $1-10\text{ s}^{-1}$ at ambient temperatures. Quantitative analysis of variable temperature data for the coprohemin II complex yielded $E_a \sim 17\text{ kcal/mol}$ and $A \sim 6 \times 10^{12}$ or $\Delta H^\ddagger \sim 17\text{ kcal/mol}$, $\Delta S \sim 0$, indicating that the reorientation takes place within the folded holoprotein. The rate of rotational hopping of the dipropionate hemin was found ~ 3 times faster in horse than sperm whale metMbCN, indicating that the propionate residue CD3 salt bridge is more stable for the Arg CD3 in sperm whale than the Lys CD3 in horse myoglobin, which supports previous conclusions reached on the basis of labile proton exchange and preferential formation of propionate salt bridges in the two proteins.

Introduction

The strong binding of the prosthetic group to the polypeptide chain of myoglobin (Mb) involves a number of interactions that contribute to the stability of the folded holoprotein. These include the bond between the proximal His F8 imidazole and the iron, salt bridges between the protein and the two heme propionates, and strong hydrophobic or van der Waals interactions between the large heme π system and the hydrophobic side chains that predominantly line the pocket.¹⁻³ These latter interactions appear

to provide the dominant stabilization, as witnessed by the stable and structurally minimally perturbed proteins found when either the iron is removed from the heme center^{4,5} or one or both of the salt bridges are abolished.^{6,7} Even large aromatic dyes bind relatively strongly in the heme pocket.⁸ In spite of the tight binding of the heme, the Mb pocket exhibits remarkable flexibility

(1) Antonini, E.; Brunori, M. *Hemoglobin and Myoglobin in Their Reaction with Ligands*; North Holland Publishing: Amsterdam, 1971; pp 55-97.

(2) Takano, T. *J. Mol. Biol.* **1977**, *110*, 537-568. Phillips, S. E. V. *J. Mol. Biol.* **1980**, *192*, 531-534. Kuriyan, J.; Wilz, S.; Karplus, M.; Petsko, G. A. *J. Mol. Biol.* **1986**, *192*, 133-154.

(3) Evans, S. V.; Brayer, G. D. *J. Biol. Chem.* **1987**, *262*, 4263-4268.
(4) Jameson, D. M.; Gratton, E.; Weber, G.; Alpert, B. *Biophys. J.* **1984**, *45*, 793-803.

(5) La Mar, G. N.; Pande, U.; Hauksson, J. B.; Pandey, R. K.; Smith, K. M. *J. Am. Chem. Soc.* **1989**, *111*, 485-491.

(6) Tamura, M.; Asakura, T.; Yonetani, T. *Biochim. Biophys. Acta* **1973**, *295*, 467-479.

(7) La Mar, G. N.; Emerson, S. D.; Lecomte, J. T. J.; Pande, U.; Smith, K. M.; Craig, G. C.; Kehres, L. A. *J. Am. Chem. Soc.* **1986**, *108*, 5568-5573.

(8) Macgregor, R. B.; Weber, G. *Nature (London)* **1986**, *319*, 70-73.

as reflected in a number of dynamic properties.⁹⁻¹⁴ This dynamic picture of the pocket is a necessity for rationalizing the access of ligands to the binding site,¹⁰ since the ground-state structures of Mb, as visualized by X-ray crystallography, do not reveal any ligand entry pathways.^{2,3} ¹H NMR spectroscopy has been particularly successful in probing heme pocket dynamics by monitoring diverse rate processes that relate to the dynamic stability of the heme pocket: labile proton exchange of proximal and distal residues,¹¹ reorientation of heme pocket aromatic side chains,¹² reorientation of the whole heme about one of its pseudo-two-fold axes,¹³ and rotational "hopping" of the heme about an intact His-iron bond.¹⁴

The first three processes have been described in detail for the standard O₂ binding reference hemoprotein, sperm whale Mb, at least in the paramagnetic met derivatives,¹¹⁻¹³ and comparative data exist for related genetic variants that reflect structural features unique to particular proteins.¹⁵⁻¹⁷ Much less is known about the dynamic properties of the heme with respect to rotation about the iron-His bond. This phenomenon was first qualitatively described for Mb reconstituted with synthetic hemes that did not possess any propionate side chains, and hence the rotational mobility was attributed to the absence of propionate-protein links.^{14,18} We have provided preliminary ¹H NMR data^{19,20} that such rotational mobility may be a general property of the heme pocket, even when propionate-protein links are present. Thus, reconstitution of Mb with a number of hemes possessing a wide variety of substitution patterns involving solely propionates and methyls revealed that not only can the heme pocket accommodate a heme propionate at virtually any nonnative site in the protein matrix, but in a number of cases alternate occupation of propionates may exist whose interconversion can be readily monitored by dynamic line broadening or saturation-transfer ¹H NMR.^{19,20} The quantitative description of such rotational hopping could provide important information on the energetics of the noncovalent heme-protein interactions. In the previous systems we have investigated,^{19,20} the difficulties encountered in separating the thermodynamics from the dynamics of the interconversion of alternate rotational sites, coupled with the spectral resolution problems that arose when two distinct molecular species were present, precluded the characterization of the activation parameters. To facilitate the quantitative description as the energetic of such rotational hopping, it is convenient to monitor the process on hemes that are centrosymmetric, which guarantees that the potential alternate sites for a given heme methyl are equally populated; i.e., the thermodynamics involving the alternate sites are temperature independent.

We base such centrosymmetric hemes on the (propionate)_n-(methyl)_{8-n}porphine-iron(III) skeleton. Two such hemes are members of the four coprohemin-type isomers,²¹ which possess

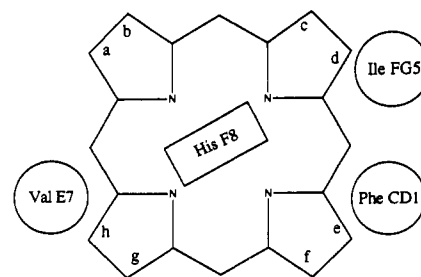
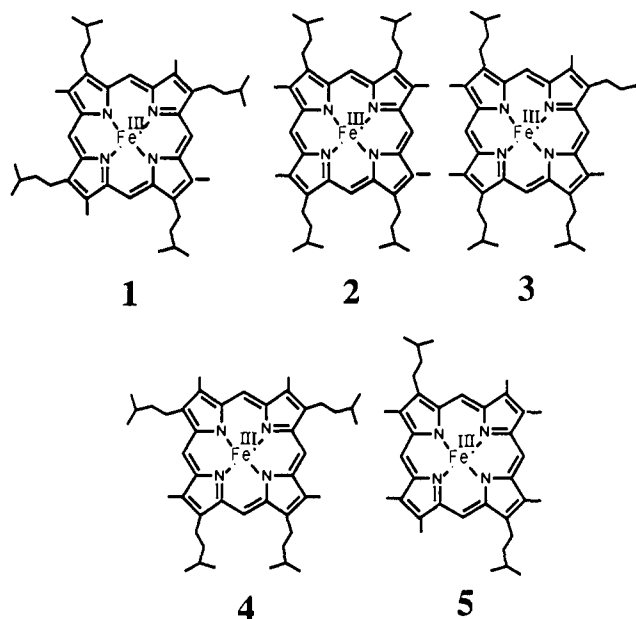


Figure 1. Schematic representation of the hemin skeleton in the pocket of myoglobin, with the position of substituents labeled in a protein-based labeling scheme, a-h, that relates position to proximity of the pocket residues indicated. In native Mb, positions a, c, e, and h are occupied by methyls, positions b and d by vinyls, and positions f and g by propionate groups.

four propionates, one on each pyrrole, with the centrosymmetric isomers coprohemin I (**1**) and coprohemin II (**2**). Intercalation of these two hemes will introduce four propionates into the heme pocket. For completeness, we also consider the other two members, coprohemin III (**3**) and coprohemin IV (**4**). The coprohemin, in addition to providing ideal cases for rotational hopping, serve as further probes of the ability of the heme pocket for accommodating polar side chains in the hydrophobic interior.²⁰ The dipropionate hemin,²² **5**, has been shown²⁰ to intercalate cleanly



- (9) Gurd, F. R. N.; Rothgeb, T. M. *Adv. Protein Chem.* **1979**, *33*, 73-105.
 Karplus, M.; McCammon, A. D. *CRC Crit. Rev. Biochem.* **1981**, *9*, 293-349.
 Debrunner, P. G.; Frauenfelder, H. *Annu. Phys. Chem.* **1982**, *33*, 283-299.
 (10) Case, D. A.; Karplus, M. *J. Mol. Biol.* **1979**, *132*, 343-368.
 (11) Lecomte, J. T. J.; La Mar, G. N. *Biochemistry* **1985**, *24*, 7388-7395.
 (12) Emerson, S. D.; Lecomte, J. T. J.; La Mar, G. N. *J. Am. Chem. Soc.* **1988**, *110*, 4176-4182.
 (13) La Mar, G. N.; Toi, H.; Krishnamoorthi, R. *J. Am. Chem. Soc.* **1984**, *106*, 6395-6401.
 (14) Neya, S.; Funasaki, N. *Biochim. Biophys. Acta* **1988**, *952*, 150-157.
 (15) Kong, S. B.; Cutnell, J. D.; La Mar, G. N. *J. Biol. Chem.* **1983**, *258*, 3843-3849. Krishnamoorthi, R.; La Mar, G. N.; Mizukami, H.; Romero, A. *J. Biol. Chem.* **1984**, *259*, 8826-8831. Lecomte, J. T. J.; La Mar, G. N.; Winterhalter, K.; Smit, J. D. G. *J. Mol. Biol.* **1985**, *180*, 357-370. Peyton, D. H.; La Mar, G. N.; Pande, U.; Ascoli, F.; Smith, K. M.; Pandey, R. K.; Parish, D. W.; Bolognesi, M.; Brunori, M. *Biochemistry* **1989**, *28*, 4880-4887.
 (16) Krishnamoorthi, R. Ph.D. Thesis, University of California, Davis, 1982.
 (17) Yamamoto, Y.; La Mar, G. N. *Biochemistry* **1986**, *25*, 5288-5297.
 Belleli, A.; Foon, R.; Ascoli, F.; Brunori, M. *Biochem. J.* **1987**, *246*, 787-789.
 (18) Neya, S.; Funasaki, N. *J. Biol. Chem.* **1987**, *262*, 6725-6728.
 (19) Hauksson, J. B.; La Mar, G. N.; Pandey, R. K.; Rezzano, I. N.; Smith, K. M. *J. Am. Chem. Soc.* **1990**, *112*, 6198-6205.
 (20) Hauksson, J. B.; La Mar, G. N.; Pandey, R. K.; Rezzano, I. N.; Smith, K. M. *J. Am. Chem. Soc.* **1990**, *112*, 8215-8224.
 (21) Abraham, R. J.; Barnett, G. H.; Bretschneider, E. S.; Smith, K. M. *Tetrahedron* **1973**, *29*, 553-560.

in the heme pocket of sperm whale Mb. Detailed ¹H nuclear Overhauser effect (NOE)²³ studies on the metMbCN complex of **5** demonstrated²⁰ the unique orientation in the heme pocket which has the two propionates positioned at points b and f in the heme labeling scheme referenced to the protein matrix, as shown in Figure 1. We present herein a structural ¹H NMR characterization of the sperm whale metMbCN complex reconstituted with the coprohemin **1-4** and an analysis of the rate of rotational hopping of the hemes **1, 2,** and **5** within the heme pocket. The structural characterization will be carried out by NOE methods that relate the position of heme methyls to fixed points on the protein matrix identified by the symbols a-h (Figure 1), defined by easily identified and characteristically hyperfine shifted heme pocket amino acid residues.^{7,19,20} The dynamics of rotational hopping are pursued by saturation-transfer²⁴ ¹H NMR between

(22) Pandey, R. K.; Rezzano, I. N.; Smith, K. M. *J. Chem. Res.* **1987**, 2172-2192.

(23) Neuhaus, D.; Williamson, M. *The Nuclear Overhauser Effect*; VCH Publishers: New York, 1989; Chapter 2.

(24) Sandström, J. *Dynamic NMR Spectroscopy*; Academic Press: New York, 1981; Chapter 5.

exchanging sites, i.e., methyls on adjacent pyrroles in fourfold symmetric hemins **1** or methyls on *trans*-pyrroles in two-fold symmetric hemins **2** and **5**.

Experimental Section

The four coproporphyrin-type isomers I–IV and their iron complexes, **1–4**, were synthesized according to known literature methods,^{21,25} hemin **5** has been described earlier.²⁰ Sperm whale and horse myoglobins were purchased from Sigma Chemical Co. and used without further purification. Apomyoglobin (apoMb) from both proteins was prepared and purified by standard methods.²⁶ The reconstitution of apoMb with various hemins was performed according to the procedure described previously.^{5,7,19,20} The apoMb (~30 mg) was dissolved in ~2–3 mL of ¹H₂O solution containing 0.1 M phosphate buffer at pH 6.5. The hemins were dissolved in 0.5 mL of H₂O solution containing a small amount of KCN. The reconstitution was monitored optically with the Soret absorption band at 410 nm with a small amount of aliquots of hemin and apomyoglobin solution; the sharp breaks at 1:1 molar ratio verified the stoichiometric incorporation of the hemins within the Mb pocket.²⁷ After reconstitution, the holoprotein solutions were passed through a Sephadex G-25 column, when necessary, and exchanged with ²H₂O several times by using an Amicon ultrafiltration cell (YM5 membrane) at 4 °C. The final 0.5 mL of protein solution was centrifuged to remove any precipitate and transferred to a 5-mm NMR tube. The protein was 1–2 mM. The reported pH values are meter readings uncorrected for the isotope effect. The solution pH was adjusted with 0.1 M ²HCl or NaO²H.

The ¹H NMR experiments were performed on a Nicolet NM-500 (500 MHz) spectrometer. Typically ~3 × 10³ transients were acquired with a 1-s relaxation delay, using 8192 points over a 12-kHz bandwidth. A 200–500-ms decoupler pulse was used to presaturate the residual solvent line. The resulting free induction decays were apodized by 20 Hz to improve the signal to noise ratio. The NOE and saturation-transfer difference spectra were obtained by subtracting on- and off-resonance irradiation traces; the spectra were acquired in double precision and interleaved fashion. The NOE and saturation-transfer experiments were performed at variable irradiation times to ensure that steady state is achieved. The effective selective spin–lattice relaxation time, $\rho(\text{eff})$, was measured by the standard selective saturation–recovery methods using the decoupler to saturate the desired resonance ≥80%. The data were analyzed by the initial slope of the standard semilogarithmic plots with Nicolet software. The chemical shifts are reported in parts per million, relative to 2,2-dimethyl-2-pentane-5-sulfonate (DSS) via the residual solvent line.

The saturation factor of resonance *j*, F_j , is given by^{11,24}

$$F_j = \frac{I_j}{I_\rho} = \frac{\rho_j}{\rho_j(\text{eff})} \quad (1)$$

where I_j and I_ρ are the intensities of resonance *j* when resonance *i* is saturated and at equilibrium, respectively, and ρ_j and $\rho_j(\text{eff})$ are the longitudinal relaxation rates of spin *j* in the absence and presence of chemical exchange between sites *i* and *j*, k_{ij} , with

$$\rho_j(\text{eff}) = \rho_j + k_{ij} \quad (2)$$

The intensity of peak *j* in the difference trace between off- and on-resonance saturation of peak *i* yields directly $1 - F_j$, and the initial slope of the selective saturation–recovery experiment of peak *j* yields $\rho_j(\text{eff})$. This allows determination of the exchange rate from eqs 1 and 2 via

$$k_{ij} = \rho_j(\text{eff})(1 - F_j) \quad (3)$$

Results

Structures of Coprohemins metMbCN Complexes. The ¹H NMR spectra of the sperm whale metMbCN complex of coprohemins I (**1**) at 25 and 5 °C at pH 5.6 are illustrated in parts A and C of Figure 2. The additional low-field resonance obtained in 50% ¹H₂O/²H₂O, labeled H_p , directly assignable^{11,15} to the proximal His F8 ring NH, is shown in the inset to trace A. The distal His E7 N_εH, observed further downfield at alkaline pH in native metMbCN, is exchange broadened beyond detection, as also observed in native metMbCN.¹¹ Saturation of the characteristic Ile FG 5 C_γH peak H_z at -7 ppm identifies the Ile FG 5 C_γH₃ (M_x) and C_δH₃ (M_y) signals (not shown); irradiation of the rapidly

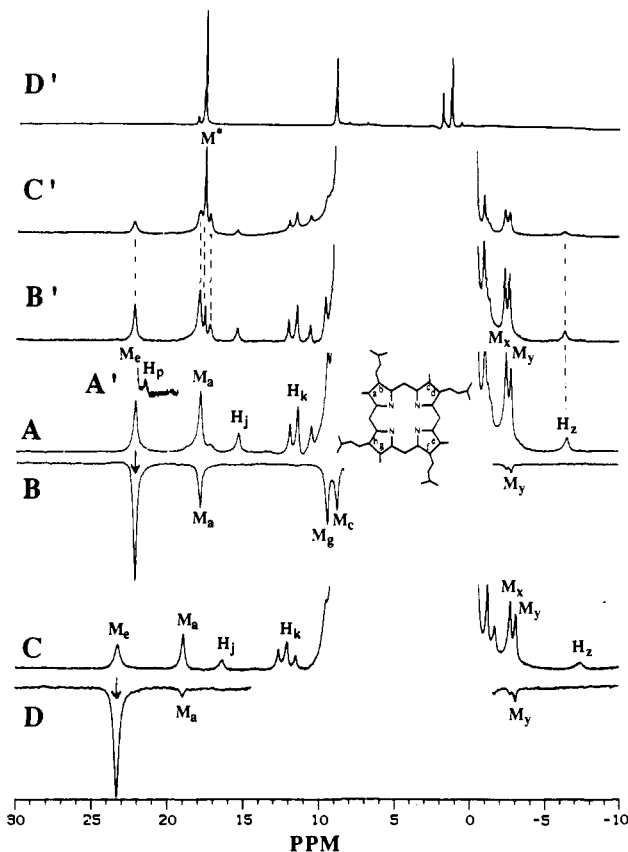


Figure 2. 500-MHz ¹H NMR spectrum of sperm whale metMbCN reconstituted with coprohemins I, **1**, in ²H₂O, pH 5.6 at (A) 25 and (C) 5 °C. The inset (A') shows a portion of the trace at 25 °C in ¹H₂O with the labile proton peak H_p . Saturation of M_e at (B) 25 and (D) 5 °C; note temperature-independent NOE to Ile FG 5 C_γH₃ (M_x) that identifies a methyl position *e* and temperature-dependent saturation transfer to methyl peaks M_a , M_c , and M_g . 25 °C NMR trace at (B') pH 6.4 and (C') pH 7.4; note loss of peaks M_i and H_i and appearance of peaks M^* and H^* , identical with those of the biscyano complex of free coprohemins I (D').

relaxing Phe CD1 C_βH peak H_j yields the characteristic NOEs to Phe CD1 C_βHs (H_k , not shown), as detailed previously for numerous metMbCN complexes.^{7,8,12,19,20,28} Saturation of the methyl signal M_e at 5 °C yields the NOE to Ile FG 5 M_y (Figure 2D) that uniquely identifies a methyl at position *e* in the protein matrix (Figure 1). This unambiguously assigns the orientation with the four propionates at positions b, d, f, and h (Figure 1), the positions occupied by 2-vinyl, 4-vinyl, 6-propionate, and 8-methyl of native protohemin in the crystal structure of Mb.²

The ¹H NMR spectra of the sperm whale metMbCN complex of coprohemins II (**2**) in ²H₂O at 25 °C and pH 6.0 is illustrated in Figure 3A; the inset shows the His F8 ring NH signal,¹¹ H_p , in 50% ¹H₂O/²H₂O. Irradiation of the characteristically shifted and relaxed Ile FG 5 C_γH signal H_z and Phe CD1 C_βH peak H_j again identifies^{7,12,19,20,28} the two Ile FG 5 methyls, M_x and M_y , and Phe CD1 C_βH peak H_k (not shown). Saturation of methyl peak M_e (Figure 3B) exhibits the NOE to Ile FG 5 (C_δH₃ peak M_y) that is diagnostic of a methyl at position *e* in Figure 1. Hence, the unique orientation is identified as that with propionates at positions b, c, f, and g in the protein matrix (Figure 1), occupied by 2-vinyl, 3-CH₃, and the 6- and 7-propionates of native protohemin in the Mb crystal structures.

The 25 °C ¹H NMR trace of sperm whale metMbCN reconstituted with coprohemins III (**3**) at pH 5.9 is illustrated in Figure 4A. The diagnostic Phe CD1 and Ile FG5 signals are again identified by NOEs from Phe CD1 C_βH peak H_j and Ile FG5 C_γH peak H_z (not shown). Saturation of methyl peak M_e yields the

(25) Smith, K. M.; Fujinari, E. M.; Langry, K. C.; Parish, D. W.; Tabba, H. D. *J. Am. Chem. Soc.* **1983**, *105*, 6638–6646.

(26) Teale, F. W. J. *Biochim. Biophys. Acta* **1959**, *35*, 563.

(27) Asakura, T.; Yonetani, T. *J. Biol. Chem.* **1969**, *244*, 4573–4579.

(28) Ramaprasad, S.; Johnson, R. D.; La Mar, G. N. *J. Am. Chem. Soc.* **1984**, *101*, 5330–5335.

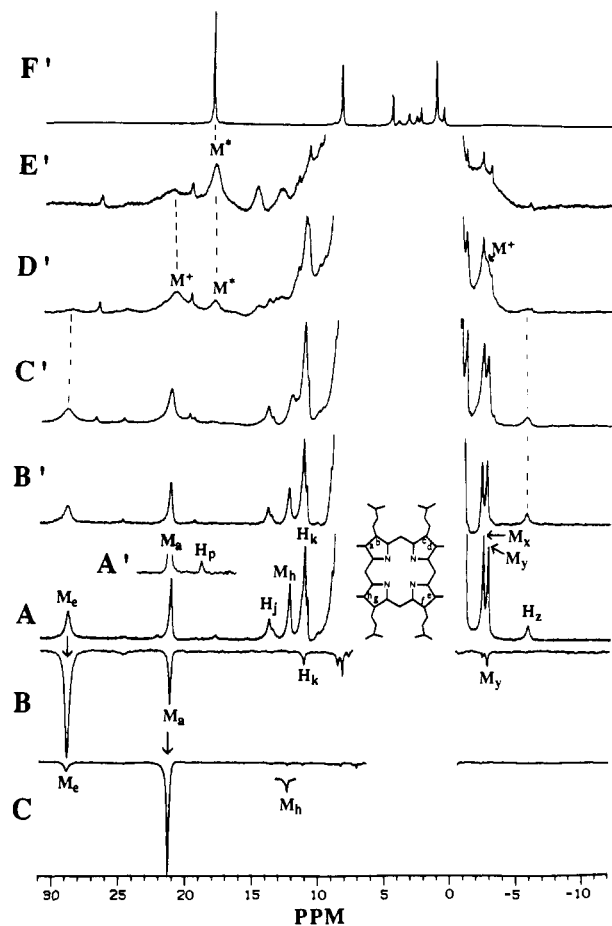


Figure 3. (A) 500-MHz ^1H NMR spectrum of sperm whale metMbCN reconstituted with coprohemins II, **2**, in $^2\text{H}_2\text{O}$ at 25 $^\circ\text{C}$, pH 6.0. The inset (A') shows a portion of the trace in $^1\text{H}_2\text{O}$ with the labile proton peak H_p . (B) Saturate M_e ; note NOEs to Ile FG 5 $\text{C}_\alpha\text{H}_3$ (M_y) and Phe CD1 C_βH_s (H_c), as well as saturation transfer to M_a . (C) Saturate M_a ; note NOE to M_e and reciprocal saturation transfer to M_e . The influence of pH at 25 $^\circ\text{C}$ is shown in (B') pH 7.0, (C') pH 7.7, (D') pH 8.1, and (E') pH 8.6; note first appearance of peak labeled M^* before the first appearance of a peak M^* that is the same as that for the biscyano complex of free coprohemins II (F').

NOE to Ile FG5 M_y (Figure 4B) that identifies a methyl at position e in the protein matrix (Figure 1). Irradiation of methyl peak M_h yields NOEs in the upfield region to Val E11 C_αH (H_c) diagnostic for position h in Figure 1; moreover, the small NOE to the remaining resolved methyl peak M_a demands methyls M_a and M_h are adjacent to the same meso position,⁷ and thereby uniquely identifies the heme orientation as that with propionates in the protein matrix at positions b, d, f, and g (Figure 1), those normally occupied by 2-vinyl, 4-vinyl, and the 6- and 7-propionates of native protohemin. Addition of coprohemins IV (**4**) to apoMb in the pH range 5.5–8.0 yielded only optical and ^1H NMR spectra that were the superposition of the individual components and hence gave no evidence for the incorporation of hemin **4** into the heme cavity.

pH Influences. The effect of pH on the ^1H NMR spectral parameters of sperm whale metMbCN reconstituted with coprohemins I (**1**) is illustrated in parts A, B', and C' of Figure 2. Raising the pH leaves the shifts of the structurally characterized low pH holoprotein unaffected, but the intensity of the peaks diminishes and a new sharp resonance, M^* , appears and grows in intensity at 18 ppm. This resonance, as well as a parallel peak at 9.2 ppm, H^* , are identical with the two peaks observed for the biscyanocoprohemins I complex in $^2\text{H}_2\text{O}$ (Figure 2D'). Integration of the single methyl peak M_e and the free hemin four-methyl peak, M^* , as a function of pH yields a $\text{pK} \sim 7.8$. The coprohemins II (**2**) complex of sperm whale metMbCN exhibits a more complex pH behavior, as illustrated in Figure 3A,B'–E'. The lines for the

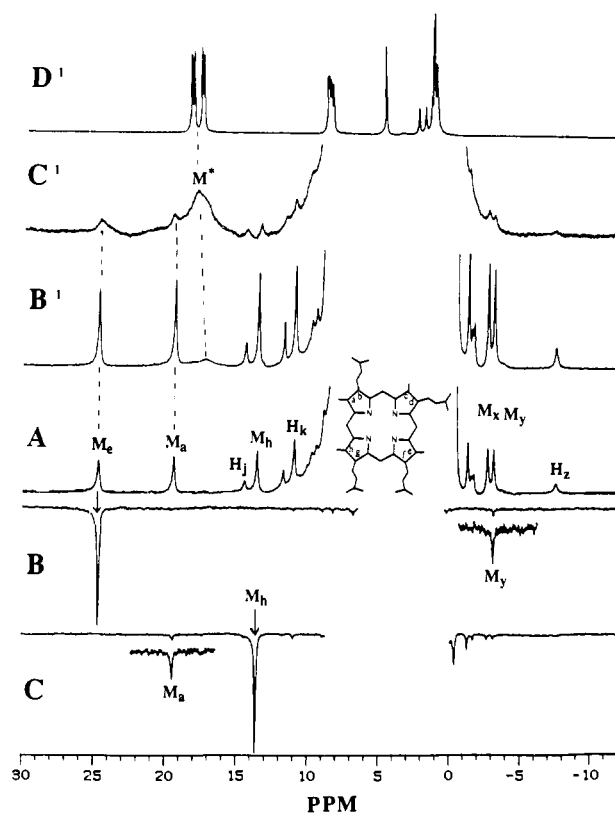


Figure 4. (A) 500-MHz ^1H NMR spectrum of sperm whale metMbCN reconstituted with coprohemins III, **3**, in $^2\text{H}_2\text{O}$ at 25 $^\circ\text{C}$, pH 5.6. (B) Saturate M_a ; note NOE to Ile FG 5 $\text{C}_\alpha\text{H}_3$ (M_y). (C) Saturate M_e ; note NOE to M_a . NMR traces at 25 $^\circ\text{C}$ as pH is elevated: (B') pH 7.8; (C') pH 8.5; note loss of intensity of peaks M_e and H_c and appearance of composite set of peaks, M^* , at the positions for the methyls in the biscyano complex of free coprohemins III, **3** (D').

holoprotein diminish in intensity when the pH is raised, first giving rise to an intermediate with an intense peak at 20 ppm, M^* , just upfield of the M_a peak, as well as an apparent protein peak at ~ 3 ppm, M^* (Figure 3D'). At higher pH, a new pair of broad resonances is observed, one of which, M^* , has the same chemical shift as methyl in the biscyano complex of coprohemins II (**2**) (Figure 3F'). The presence of more than two species precludes determination of a pK ; however, the loss of half of the original M_e intensity occurs at pH ~ 7.9 .

Raising the pH of the solution of the coprohemins III (**3**) complex of sperm whale metMbCN leads to a loss of intensity of the peaks for the holoprotein, and the appearance of a broadened composite peak, M^* (Figure 4C'), centered at the position of the resolved set of four methyl resonances observed for the biscyano complex of coprohemins III (**3**). Estimates of the relative areas of the one-methyl peak, M_e , and the four-methyl composite, M^* , at 17 ppm as a function of pH, yields a $\text{pK} \sim 8.3$. Previous pH studies of the sperm whale metMbCN complexes of hemin **5** had shown²⁰ the spectral parameters to be completely pH independent in the region pH 6–10.

Saturation-Transfer Studies. It is noted that when a heme methyl peak is saturated at 25 $^\circ\text{C}$ for each of the sperm whale metMbCN complexes of coprohemins I (**1**) (Figure 2C) or coprohemins II (**2**) (Figure 3B,C), in addition to NOEs to the assigned protein peaks that determine the orientation in the heme pocket, significant saturation transfer is observed by each of the three other methyls for the coprohemins I complex (**1**) (Figure 2B) and between the two resolved methyl M_a and M_e for the coprohemins II complex (**2**) (Figure 3B,C). The degree of saturation transfer is dramatically reduced at low, and increased at high, temperature, indicating that we are monitoring a chemical exchange phenomenon²⁴ that scrambles the four methyls of coprohemins I (**1**) and interchanges the M_e with M_a environments of coprohemins II (**2**). For the coprohemins II complex of sperm

Table I. Chemical Shift for MetMbCN Complexes of Hemins 1–3 and 5^a

peak assignment ^b	sperm whale metMbCN				horse metMbCN hemin 5
	hemin 1	hemin 2	hemin 3	hemin 5	
M _a	17.9	21.3	19.4	17.8	17.8
M _c	8.9		c	8.2	8.6
M _d		8.6		9.0	9.2
M _e	22.2	28.9	24.7	21.0	20.7
M _g	9.8			9.8	10.2
M _h		12.3	13.6	11.9	12.5
Phc CD 1 C ₅ H	14.9	14.8	14.5	15.8	15.8
C ₁ H ₅	11.8	11.2	11.0	11.3	11.9
Ilc FG 5 C ₇ H ₃	-2.4	-2.4	-2.7	-2.5	-2.5
C ₆ H ₃	-2.7	-2.8	-3.1	-2.9	-3.0
C ₇ H	-6.5	-5.8	-7.5	-6.5	-6.3
His F8 N _δ H	21.4	18.9	c	21.8	c
His E7 N _ε H	d	d	d	25.4	c

^aShifts in ppm from DSS at 25 °C in ²H₂O; pH ~6.0 for hemins 1–3; pH ~8.0 for hemin 5. ^bPeaks labeled according to position occupied in protein-based labeling system depicted in Figure 1. ^cNot located. ^dExchange broadened beyond detection.

whale metMbCN, the saturation factors M_c → M_a and M_c → M_e are independent of pH in the range 5.9–6.6. Measurement of the saturation factor, *F*, as well as the selective effective relaxation rate, ρ_i(eff), for both M_c and M_a peaks as a function of temperature in the range 15–35 °C yields the data in Table II. The difference in the M_a → M_c and M_c → M_a saturation factors reflects the relative relaxation rates. Arrhenius and Eyring plots for the exchange rates obtained via eq 3 yield the straight lines in Figure 5 which yield the activation energy, E_a = 16.7 ± 2.1 kcal/mol, and the pre-exponential factor, 6 × 10¹², and Δ*H*[‡] = 17.2 ± 2.1 kcal/mol and Δ*S*[‡] = -5 ± 5 entropy units, respectively. Because of the need to treat four-site exchange, and the inability to measure all four needed selective relaxation rates, the exchange rate for the coprohemin I (1) complex was not analyzed quantitatively.

The ¹H NMR spectra of sperm whale metMbCN reconstituted with the dipropionate hemin 5 at pH 8.0 had been reported previously,²⁰ leading to the assignment of methyls at 35 °C shown in Figure 6A, where the subscript again refers to the position of the methyl in the protein matrix, as shown in Figure 1. The inset to Figure 6 shows the additional hyperfine-shifted labile proton peaks that arise from the distal His E7 N_εH (H_q) and proximal

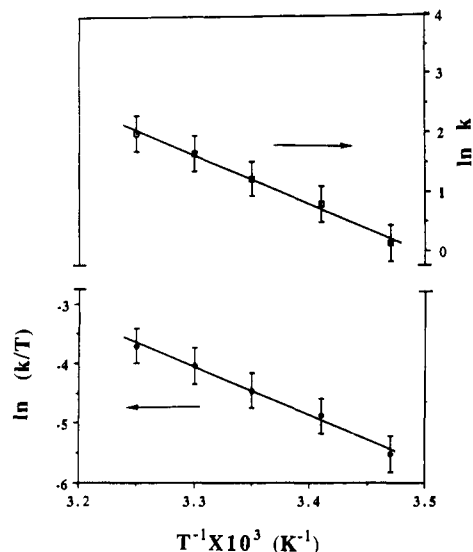


Figure 5. Arrhenius ($\ln k$ vs T^{-1}) and Eyring ($\ln k/T$ vs T^{-1}) plots for rotational hopping of coprohemin 1, 2, in sperm whale metMbCN. The fitted lines yield $E_a = 16.7 \pm 2.1$ kcal/mol, $A = 6 \times 10^{12}$, and $\Delta H^\ddagger = 17.2 \pm 2.1$, $\Delta S^\ddagger = -5 \pm 5$ entropy units.

His F8 N_δH (H_p); at this pH, the His E7 peak is resolved.¹¹ Upon saturation of M_c at 40 °C and pH 8.0, we observe, in addition to the previously reported²⁰ NOEs, very small but detectable saturation transfer to M_a (Figure 6B); the reverse process is also observed (Figure 6C), and both processes are undetectable below 35 °C. The 500-MHz ¹H NMR trace of the horse metMbCN complex of hemin 5 at pH 8.0 is illustrated in Figure 6D; it is essentially identical with that of the sperm whale complex in Figure 6A and hence can be assumed to have the same heme orientation and assignments.²⁰ Saturation of methyls M_c (Figure 6E) and M_a (Figure 6F) leads to reciprocal saturation transfer that is suppressed at lower temperatures. The selective effective relaxation rates for peak M_a was determined for each protein, and the exchange rates were determined by using eq 3. The rate data are collected in Table II.

Limits to the exchange rate of the rapidly relaxing His F8 ring labile proton: signal H_p of the coprohemin II (2) complex of sperm whale metMbCN were determined from the intensity change when the bulk water signal was saturated in 50% ¹H₂O, as described

Table II. Saturation Factors, Relaxation Rates, and Hemin Hopping Rates for MetMbCN Complexes Reconstituted with Various Centrosymmetric Hemins

Coprohemin II in Sperm Whale Mb ^a						
<i>T</i> , °C	1 - <i>F</i> _a	ρ _a (eff)	<i>k</i> _{a→c} ^c	1 - <i>F</i> _c	ρ _c (eff)	<i>k</i> _{a→c} ^c
15	0.08 ± 0.02	14 ± 2	1.1 ± 0.4	0.05 ± 0.02	25 ± 3	1.2 ± 0.3
20	0.14 ± 0.02	14 ± 2	1.9 ± 0.5	0.10 ± 0.02	24 ± 3	2.6 ± 0.5
25	0.26 ± 0.03	13 ± 2	3.2 ± 0.7	0.16 ± 0.02	23 ± 2	3.6 ± 0.7
30	0.39 ± 0.04	13 ± 2	5.1 ± 0.9	0.25 ± 0.03	22 ± 2	5.6 ± 0.9
35	0.58 ± 0.06	12 ± 2	6.7 ± 1.0	0.39 ± 0.04	22 ± 2	8.4 ± 1
Coprohemin I in Sperm Whale Mb ^a						
<i>T</i> , °C	1 - <i>F</i> _a	ρ _a (eff)		1 - <i>F</i> ₂	ρ _c (eff)	
5	0.05 ± 0.02	<i>d</i>		0.07 ± 0.02	<i>d</i>	
15	0.13 ± 0.02	<i>d</i>		0.16 ± 0.02	<i>d</i>	
20	0.20 ± 0.03	<i>d</i>		0.25 ± 0.03	<i>d</i>	
25	0.30 ± 0.04	11 ± 2		0.35 ± 0.04	14 ± 2	
35	0.47 ± 0.05	<i>d</i>		0.60 ± 0.006	<i>d</i>	
Hemin 5 in Sperm Whale Mb ^b						
<i>T</i> , °C	1 - <i>F</i> _a	ρ _a (eff)	<i>k</i> ^c	1 - <i>F</i> _c	ρ _c (eff)	
40	0.03 ± 0.01	14 ± 2	0.9 ± 0.3	0.03 ± 0.01	<i>d</i>	
Hemin 5 in Horse Mb ^b						
<i>T</i> , °C	1 - <i>F</i> _a	ρ _a (eff)	<i>k</i> ^c	1 - <i>F</i> _c	ρ _c (eff)	
40	0.11 ± 0.03	14 ± 2	2.8 ± 0.5	0.09 ± 0.03	<i>d</i>	

^aData taken at pH 5.9. ^bData taken at pH 8.0. ^cRates calculated via eq 3. ^dRelaxation rate not determined.

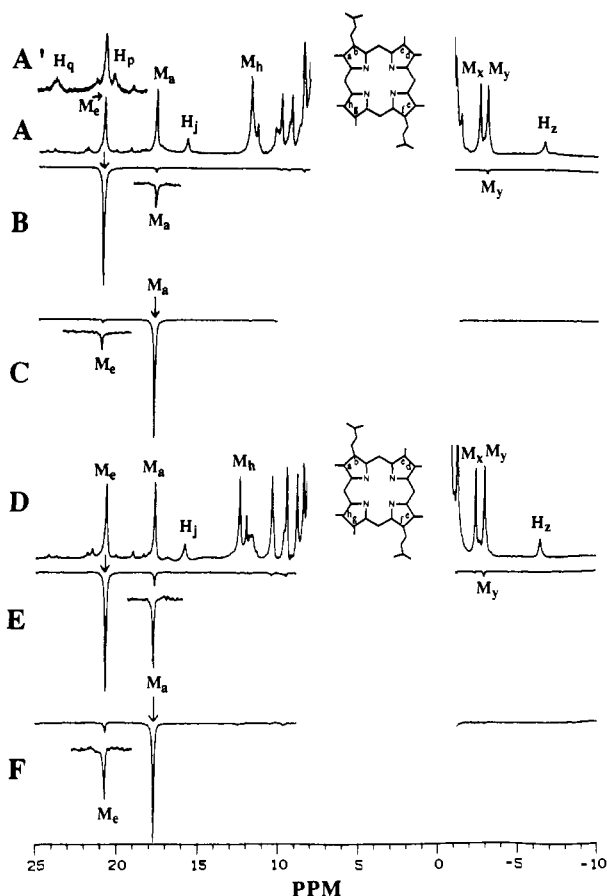


Figure 6. 500-MHz ^1H NMR spectra of metMbCN complexes of hemin **5**, in $^2\text{H}_2\text{O}$ at 40°C , pH 8.0, for (A) sperm whale Mb, with previously determined assignments,²⁰ and (D) horse Mb, with assignments determined by analogy to the trace in (A). The inset (A') shows a portion of the trace for the sperm whale complex in $^1\text{H}_2\text{O}$ with the labile proton peaks H_p and H_q . Saturate M_e for (B) sperm whale Mb and (E) horse Mb; note previously characteristic NOEs to M_y as well as saturation transfer to M_a . Saturate M_a for (C) sperm whale Mb and (F) horse Mb; note reciprocal saturation transfer to M_e .

in detail elsewhere.¹¹ The saturation factor was observed as 1.00 ± 0.05 at both pH 6.0 and 7.0. With the observed relaxation rate of 40 s^{-1} for signal H_p , eqs 1 and 2 dictate that exchange rates with bulk water, k^* , be $< 2\text{ s}^{-1}$ at 25°C at both pH 6.0 and 7.0.

Discussion

Heme Orientation. Previous studies of sperm whale metMbCN reconstituted with isomeric (propionate)_{*n*}(methyl)_{*8-n*}porphine-iron(III) with $n = 1, 2,$ or 3 revealed that,^{19,20} in addition to the native 6,7-propionate sites at positions f and g in Figure 1, the heme propionates have a substantial affinity for position b (the native 2-vinyl position), where the propionate likely intercalates with the "xenon" hole,² with reduced but detectable affinity for positions k (native 8- CH_3) and d (native 4-vinyl) in Figure 1. The positions which least readily accommodated propionates are positions a (native 1- CH_3), c (native 3- CH_3), and e (native 5- CH_3) in Figure 1. The present studies with the coprohemin-type isomers reveal that, depending on their position, even four propionic acid side chains are readily accommodated within the pocket without significantly perturbing the pocket molecular and/or electronic structure, as evidenced by the characteristic hyperfine shift patterns for both heme and amino acid residues (Table 1). Coprohemin I (**1**), II (**2**), and III (**3**) each place their propionic acid side chains at positions known to accommodate propionic acid side chains readily in the previous studies:²⁰ the native f and g propionate positions, the b and d vinyl positions, and the 8- CH_3 or h position. It is noted that the most reasonable orientation of coprohemin IV (**4**) that could have been expected is that with the a and d positions, in addition to the native f and g positions, occupied by the four propionic acid side chains. That a holoprotein complex

of Mb could not be detected at any pH for coprohemin IV (**4**) dictates that the a position cannot accommodate a propionic acid side chain at the same time as the d position, so that the heme binding to the protein is considerably reduced. The present studies further confirm the remarkable resiliency of the heme pocket in accommodating the polar carboxylic acid side chains within the pocket interior.

Thermodynamics of Hemin Binding. While essentially native heme pocket structure is displayed by the sperm whale metMbCN complexes of coprohemin I–III (**1–3**) at low pH, it is also clear that elevating the pH causes a major structural change centered at pH ~ 8 for each of the hemins. For the coprohemin I complex (**1**) the ^1H NMR spectrum of the alkaline pH product is identical with that of the biscyano coprohemin I (**1**) complex (Figure 2D'). A similar conclusion is reached for the coprohemin III (**3**) complex, where the apparent free biscyano complex of **3** exhibits the appropriate chemical shifts, although the lines are broader, possibly due to aggregation or residual interaction with apoMb somewhere beside the native pocket. In the coprohemin II (**2**) metMbCN complex, some intermediate is formed near pH 8, which still retains heme **2** within the protein, as evidenced by upfield shifted apparent amino acid peak at ~ 3 ppm (Figure 3D'). At more alkaline pH, the ^1H NMR trace again exhibits a peak consistent with arising from the methyls of the free heme **2** complex (Figure 3E'). Thus, all three hemins exhibit vastly reduced binding to the apoMb at alkaline pH, with the dissociation into apoMb and heme described by $\text{pKs} \sim 7.8\text{--}8.2$, depending on the heme.

Previous studies of the pH behavior of the ^1H NMR spectra for the sperm whale metMbCN complexes of dipropionate and tripropionate isomers of (propionate)_{*n*}(methyl)_{*8-n*}porphine-iron(III) had revealed that,²⁰ while the f- and g-positioned propionic acid side chains exhibit "normal" $\text{pKs} \leq 5.3$, the propionic acid pK for position b is 8–10 and that for position d is ~ 8 . The remarkable elevation of the pK by 4–5 units results in a 5.5–6.9 kcal/mol destabilization of the total protein–heme interaction. Thus, while the total heme binding energy is large enough to accommodate one propionic acid side chain at such a hydrophobic, thermodynamically unfavorable environment as at positions a, c, or d, and still retain strong binding at alkaline pH,²⁰ the introduction of two such destabilizing groups overwhelms the other binding contributions and leads to dissociation of the complex at alkaline pH. The apparent pK for heme expulsion, 8.2 for coprohemin III (**3**) is the same as that traceable previously²⁰ to the d propionic acid group. The lower pK for the dissociation of coprohemin I (**1**) relative to coprohemin III (**3**) is likely due to the less favorable placement of the propionic acid at position h in the former, as opposed to position g for the latter heme.

Heme Rotational Dynamics. The magnetization transfer between the pair of methyls for the metMbCN complexes of hemins **2** and **5**, and among all four methyls of heme **1**, must unequivocally arise from a chemical exchange process,²⁴ inasmuch as none of the pairs of connected methyls is close enough to exhibit an NOE. The saturation transfer is observed solely between the symmetry-related peaks of the prosthetic group itself, i.e., among all four of the four-fold symmetric coprohemin I (**1**) complex (Figure 2B,D) and between M_a and M_e in each of the coprohemin II (**2**) (Figure 3B) and heme **5** complexes (Figure 6). The chemical exchange origin²⁴ of the saturation transfer is directly confirmed by its strong temperature dependence.

The fact that the broad His F8 ring exchangeable resonance at 19 ppm (with $T_1 \sim 25$ ms) in the sperm whale metMbCN complex of heme **2** does not exhibit saturation transfer to bulk water dictates¹¹ that the exchange rate with bulk water is $< 2\text{ s}^{-1}$ at both pH 6.0 and 7.0. However, since exchange of the proximal His F8 ring NH is base catalyzed,¹¹ we can further conclude that the limits of pH 7.0 dictate that the rate must be $< 0.2\text{ s}^{-1}$ at pH 6. Since this exchange rate with bulk water is much slower than the observed chemical exchange rate ($3\text{--}4\text{ s}^{-1}$) of heme methyl sites, and exchange would be expected to be extremely rapid if the bond between the heme iron and His F8 were broken, we conclude that the heme reorientation is indeed occurring via hopping about an intact Fe–His F8 bond rather than by any

mechanism involving heme release. The previously characterized heme reorientation about the α,γ -meso axis, which necessarily ruptures the Fe-His bond, occurs at a rate $\sim 10^5$ slower¹³ than the presently characterized hopping.

Only the coprohemin II (2) metMbCN complex allowed measurement of all of the necessary parameters to quantitatively define the activation parameters and yields the values $E_a \sim \Delta H^\ddagger \sim 17$ kcal/mol, $A \sim 6 \times 10^{12}$, and negligible ΔS^\ddagger . These parameters are consistent with the process occurring within the folded holo-protein without major disruption of the heme pocket structure. Previously we had shown that two isomeric forms of noncentrosymmetric dipropionate, hexamethylporphyrin-iron(III), with alternate orientations in the heme pocket of sperm whale metMbCN similarly interconverted via saturation transfer.²⁰ The similar relaxation rates for hemin methyls in all of these complexes dictate that all of these hemins rotationally hop about the iron-His bond at $1-10$ s⁻¹ at ambient temperature, which is some 10^4 slower than the rates qualitatively implied by the dynamic line broadening and chemical shift averaging observed^{14,18} for the myoglobin complexes of the synthetic hemins without peripheral propionates. The difference in rates would translate into a lower rotational barrier by ~ 5.5 kcal/mol in the absence of propionates. Although the difference in rates in part reflects the steric influences due to the difference in the size of the peripheral substituents, at least part of the decreased rotational rate in the present complexes is due to the importance of the propionate salt bridges in stabilizing a fixed orientation of the hemin in its pocket. Thus, it is clear that, while propionate-protein salt bridges modulate the hopping process by stabilizing a given orientation, breaking these salt bridges must represent only a fraction of the barrier to such rotations.

Comparison of Horse and Sperm Whale Mb. Comparison of the ¹H NMR spectra of the hemin 5 complexes of sperm whale and horse metMbCN in Figure 6A,C shows that the molecular/electronic structures are essentially indistinguishable, as found earlier for the two native proteins as well as for the proteins reconstituted with a number of different hemins.^{5,11} The degree of saturation transfer, however, for essentially indistinguishable relaxation rates, is larger in the horse than sperm whale protein

by a factor ~ 3 , which translated directly to a similarly more rapid hopping rate and an implied lower activation energy of 0.6 kcal/mol for the horse protein. Hence, the heme pocket of horse metMbCN exhibits a reduced dynamic stability with respect to heme reorientation about the Fe-His F8 bond, relative to that in the sperm whale protein. The difference in the heme pocket between the two proteins is the nature of the donor residue in the salt bridge to the f-position propionate, which involves an Arg in sperm whale and a Lys in horse Mb.^{23,31} The faster rate and implied lower activation energy to rotational hopping therefore indicate that the propionate-Lys CD3 salt bridge in horse Mb is weaker than the propionate-Arg CD3 salt bridge in sperm whale Mb. This different stability of the f-propionate salt bridge in horse and sperm whale Mb had been previously detected by distinct thermodynamic processes: the preferential formation of the invariant g-propionate-His FG3 salt bridges in monopropionate heptamethylporphyrin-iron(III) reconstituted sperm whale and horse Mb¹⁹ and the lower free energy for opening the ligation channel to the protein surface, as detected by labile proton exchange,¹¹ which involves rupture of the f-propionate salt bridge.³² Thus, the three types of experiments are remarkably consistent in providing a picture of a dynamically less stable closed pocket for horse than sperm whale Mb, on the basis of three divergent dynamic and structural properties, and indicated that the rate of rotational hopping of centrosymmetric hemins provides a valuable probe for detecting differential heme pocket dynamics among Mb genetic variants and synthetic point mutants.

Acknowledgment. This research was supported by grants from the National Science Foundation (DMB 88-03611), the National Institutes of Health (HL16087, HL22252), and the Office of Naval Research (N0014-85-C-0317).

(29) Shulman, R. G.; Glarum, S. H.; Karplus, M. *J. Mol. Biol.* **1971**, *57*, 93-115.

(30) Emerson, S. D.; La Mar, G. N. *Biochemistry* **1990**, *29*, 1556-1566.

(31) Dayhoff, M. O. *Atlas of Protein Sequence and Structure*; National Biomedical Research Foundation: Washington, DC, 1972; Vol. 5.

(32) Ringe, D.; Petsko, G. A.; Kerr, D. E.; Ortiz de Montellano, R. P. *Biochemistry* **1984**, *23*, 2-4.

Characterization of Methyl α -Hydroxymethylacrylate Ether Cyclopolymer Using Nutation NMR Spectroscopy

Lon J. Mathias,*[†] Ronald F. Colletti,[†] and Anthony Bielecki[†]

Contribution from the Department of Polymer Science, University of Southern Mississippi, Hattiesburg, Mississippi 39406-0076, and Bruker Instruments, Inc., Manning Park, Billerica, Massachusetts 01821. Received August 27, 1990

Abstract: A cyclopolymer of the ether of methyl α -hydroxymethylacrylate (MHMA) was synthesized from a doubly ¹³C-labeled starting material. Nutation NMR spectroscopy was then used to determine whether the polymer contained five- or six-membered rings in the main chain generated by the cyclization step. Directly bonded ¹³C spin pairs, which are detectable by the nutation NMR experiment, can be formed only in the case of a cyclopolymer containing five-membered rings. Experimental spectra indicate only isolated ¹³C labels, suggesting that the cyclopolymer obtained under the current reaction conditions consists primarily of six-membered rings generated by strict head-to-tail addition of the methacrylate moieties.

We have previously described the facile synthesis of methyl α -hydroxymethylacrylate (MHMA)¹ and the unexpected dimerization of this material to its ether.² The cyclopolymerization of the ether to a soluble product indicated a high ratio of intramolecular over intermolecular addition of the initially formed radical intermediate.³ Detailed investigation of the reaction mechanism of both MHMA and ether formation used ²H- and

¹³C-labeled formaldehyde (Figure 1).⁴ During this study, the doubly ¹³C-labeled cyclopolymer of the ether was obtained. While formation of either the five- or six-membered ring repeat units is possible during cyclopolymerization of the ether, a model di-

[†] University of Southern Mississippi.

[†] Bruker Instruments, Inc.

(1) Kusefoglu, S. H.; Kress, A. O.; Mathias, L. J. *Macromolecules* **1987**, *20*, 2326.

(2) Mathias, L. J.; Kusefoglu, S. H. *Macromolecules* **1987**, *20*, 2039. U. S. Patent 4,889,948, Dec 26, 1989.

(3) Ingram, J. E.; Kusefoglu, S. H.; Mathias, L. J. *Macromolecules* **1988**, *21*, 545.

(4) Colletti, R. F.; Halley, R. J.; Mathias, L. J. *Macromolecules*, in press.